Global Structures of High Methoxyl Pectin from Solution and in Gels

Marshall L. Fishman,*,† Peter H. Cooke,‡ Hoa K. Chau,† David R. Coffin,† and Arland T. Hotchkiss, Jr.†

Crop Conversion Science and Engineering Research Unit and Microbial Biophysics and Residue Chemistry and Core Technologies Research Unit, Eastern Regional Research Center, Agricultural Research Service, U.S. Department of Agriculture, Wyndmoor, Pennsylvania 19038

Received August 7, 2006; Revised Manuscript Received October 25, 2006

Images of high methoxyl orange pectin deposited from solution and high methoxyl sugar acid gels (HMSAG) were obtained by atomic force microscopy (AFM) in the tapping mode. For the first time, images of pectin deposited from water revealed that the transition from pectin networks to individual molecules or aggregates thereof occurred at concentrations between 6.5 and 13.1 μg/mL. At 6.5 μg/mL, shapes included rods, segmented rods, kinked rods, rings, branched molecules, and dense circular areas. At 13.1 μg/mL, all of these shapes were integrated into networks. These same structures were discernible in pectin high methoxyl sugar acid gels. Thus one might consider pectin networks in water at concentrations in excess of 10 μg/mL to be separate fluid precursors of networks in high methoxyl sugar acid gels. Examination of AFM images revealed that gels with "uniform" distribution of strands and pores between strands had higher gel strengths as measured by a penetrometer than gels in which strands were nonuniformly distributed and were separated by large and small spaces.

Introduction

Pectin is an extremely complex polysaccharide found in the cell walls of many plants.[1] In fact it has been suggested that it is an assembly of several different polysaccharides linked together covalently.[1] Up to 17 different monosaccharides have been found in pectin from various plants but the major constituent in pectin is homogalacturonan (HG), which is (1−4) linked α-D-galacturonic acid and its methyl ester.[2] It is the presence of this constituent in abundance that distinguishes pectins from all other polysaccharides. HGs may contain pendent α-D-xylose units. Also present in pectin is rhamnogalacturonan I, which contains arabinan, galactan, and arabinogalactan side chains. These constituents account for most of the monosaccharide units present in pectin preparations even though pectin may contain other constituents.

Apparently, the complexity of pectin at the primary structure level can be translated to its behavior in solution and in gels. Earlier, experiments by high-performance size-exclusion chromatography (HPSEC),[3−5] light scattering,[6,7] electron microscopy,[8,9] and membrane osmometry in combination with end-group titrations[10] revealed that pectin formed aggregates in solution. Static and dynamic light scattering studies on pectic polysaccharides from the primary cell walls isolated from apple pomace revealed the existence of cross-linked microgels.[11] Subsequently, electron micrographs obtained by rotary shadowing of peach pectin deposited on mica from water revealed the existence of cross-linked microgels of pectin and indefinite-sized sheets of cross-linked pectin.[12,13] In these same studies, it was found that if pectin was deposited on mica from 5 mM NaCl, cross-linked networks were dissociated into branched or clustered pectin, and from 50 mM NaCl or 50% glycerol, rods, segmented rods, or kinked rods could be observed. More recent studies employing atomic force microscopy (AFM) on pectins extracted from tomatoes appeared to visualize pectins with a mixture of heterogeneous shapes.[14] An interesting feature of those studies was that branches or clusters of pectins were observed that resembled the earlier electron microscope images obtained from peach pectin.

Over the last several years we have studied the effect of heating time on the physical properties of orange and lime pectin obtained by flash extraction methods.[15,16] Characterization by HPSEC with light scattering and viscosity detection gave data consistent with the concept derived from electron microscopy that, at low heating times, pectin networks were extracted. With increased heating time, networks were reduced first to branched and then to linear molecules as described above. One objective of this study was to determine the structure of pectin extracted from oranges. A second objective was to determine the structure of pectin networks in water and in high methoxyl sugar acid gels (HMSAG). Both of these objectives were accomplished by AFM imaging of pectin dissolved in water and in HMSAG.

Experimental Section

Materials. For solution studies, fresh albedo was obtained from Florida, early Valencia oranges.[15] Immediately upon arrival in the laboratory, the flavedo was stripped manually from the skin with a potato peeler, followed by removal of the albedo with a paring knife. After the albedo was cut into small pieces (ca. 1 mm^2) it was stored at −20 °C in sealed polyethylene bags until extraction. For sugar acid gel studies, early Valencia orange albedo partially stripped of flavedo was obtained from a commercial supplier. Residual flavedo and pulp sacs were removed with a paring knife. The albedo that remained was chopped into small pieces (ca. 1 mm^2), washed with HPLC-grade water, and extracted as outlined below. To determine the accuracy of the AFM calibration, lot 08-115 rat tail collagen, type 1, was obtained from

* To whom correspondence should be addressed: tel 215-233-6450; fax 215-233-6406; e-mail mfishman@errc.ars.usda.gov.

† Crop Conversion Science and Engineering Research Unit.

‡ Microbial Biophysics and Residue Chemistry and Core Technologies Research Unit.

10.1021/bm0607729
Published on Web 01/06/2007

Upstate Cell Signaling Solutions, Lake Placid, NY. The collagen as received was dissolved in 0.02 N acetic acid at a concentration of 4 mg/ mL. The sample was serially diluted 10 000:1 with 0.05 N acetic acid to a concentration of 0.4 μg/mL.

Flash Extraction of Pectin. Orange albedo pectin for solution studies was flash-extracted with microwave heating, This method has been described in detail previously.[15] Briefly, microwave heating was performed in a model MDS-2000 microwave sample preparation system (CEM Corp., Matthews, NC). Samples were irradiated with 630 W of microwave power at a frequency of 2450 MHz. For each experiment, six equally spaced cells were placed in the sample holder, a rotating carousel. One vessel was equipped with temperature- and pressure-sensing devices that measured and controlled the temperature and pressure within the cell. Cells were loaded with 1 g of albedo dispersed in 25 mL of HCl, pH 2.Time of irradiation was 3 min followed by rapid cooling in a cold water bath to room temperature. The maximum allowed pressure level within the cell was set at 52 ± 2 psi and the maximum temperature within the cell was set at 195 °C. The extraction mixture was filtered to remove the insoluble residue. Solubilized pectin was precipitated with 70% isopropyl alcohol (IPA) and washed once with 70% IPA and once with 100% IPA. Finally, the sample was vacuum-dried at room temperature and stored in screw-capped vials until further use. The dry weight yield was 22%; degree of methylesterification (DE) 91% ± 4%, anhydrogalacturonic acid (GA) 65% ± 2%, neutral sugars (NS) 28% ± 2%, M_w (529 ± 10) × 10^3, $[\eta]_w$ 8.8 ± 0.1 dL/g, R_{gz} 47 ± 1 nm, Mark−Houwink exponent 0.50 ± 0.01. DE was determined by HPLC,[17] and GA was determined colorimetrically,[18] as was NS.[19] Physical measurements were by HPSEC with on-line light scattering and viscosity detection.[16]

Orange albedo pectin for gel studies was flash-extracted by steam injection heating.[16] The extraction vessel was a modified bacteria fermenter capable of producing 30-g batches of pectin. Five gallons (18.927 L) of pH 2.0 nitric acid (HNO_3) was preheated to 95−100 °C, followed by the addition of 774 g of wet albedo. Then the temperature was raised to 110 °C and held there for 3 min. Next the sample was rapidly cooled by use of an in-line cold water heat exchanger and filtered through Miracloth. The pectin was precipitated by adding 11.4 L of 70% IPA to the supernatant. The supernatant was stirred and allowed to stand at room temperature for $^1/_2$ h, followed by filtering. The recovered pectin was washed with 4 L of 100% IPA and placed in a −20 °C freezer overnight before being vacuum-dried the next day. The dry weight yield was 14%; DE 65% ± 2%, GA 77% ± 1%, neutral sugars (NS) 23% ± 3%, M_w (685 ± 4) × 10^3, $[\eta]_w$ 8.4 ± 0.1 dL/g, R_{gz} 43 ± 1 nm, Mark−Houwink exponent 0.47 ± 0.01. Characterization methods were as above.

Preparation of HMSAG and Determination of Gel Strength. HMSAG was prepared by dissolving 0.7 g of the pectin to be tested in 102.2 g of a 0.01 M citrate buffer. The pH of the buffer was controlled by the molar ratio of citric acid and sodium citrate. The pH values used ranged from 2.86 to 3.71, corresponding to citric acid:sodium citrate ratios of 93:7 to 70:30. The beaker containing the pectin solution was placed in a 95−98 °C water bath, and 189.0 g of sucrose was added with stirring. The mixture was covered and heated for 10 min and then poured into three 45 mL weighing bottles (38 mm i.d. × 50 mm height). Scotch tape had been placed around the top of the bottles to allow the gelling solution to be poured to a level above the rim of the bottle. The solutions were allowed to cool at ambient room temperature for 20 h. The tape was removed and the part of the gel above the rim of the bottle was removed using a cheese cutter. The final composition (w/w) of the gels was 0.25% pectin, 65% sucrose, and 35% buffer.

Gel strength was determined with a Stable Microsystems TA-XT2 texture analyzer. Probe speed was 1.0 mm/s, and the 0.5-in. diameter Delrin probe was allowed to penetrate to a depth of 15 mm. The maximum in the force penetration curve was taken as the gel strength at break. Three replicates were run for each sample.

Atomic Force Microscopy. For solution studies, samples were dissolved in HPLC-grade water and serially diluted to the desired concentration. Two microliters of the solution was pipetted onto a freshly cleaved 10 mm diameter disk of mica and air-dried. The mica was mounted in a Multimode scanning probe microscope with a Nanoscope IIIa controller, operated as an atomic force microscope in tapping mode (Veeco Instruments, Santa Barbara, CA). The thin layer of pectin adhering to the mica surface was scanned with the AFM operating in the intermittent contact mode with etched silicon probes (TESP). The spring constants for these probes were 20−100 N/m and the nominal tip radius of curvature was 5−10 nm.[20] The cantilever controls, namely, drive frequency, amplitude, gains, and amplitude set point ratio (r_{sp}), were adjusted to give images with the clearest image details. Values of r_{sp} used in this study were about 0.95. The definition of r_{sp} is given by

$$r_{sp} = A_{sp}/A_o \quad (1)$$

A_{sp} is the oscillating amplitude in contact with the sample whereas A_o is the freely oscillating amplitude (out of contact amplitude). Set point amplitudes approaching 1 correspond to light normal forces, that is, soft tapping.[21]

In the case of sugar acid gels,[20] a thin (1 mm) slice of transparent gel was cut manually from the gel with a stainless steel razor blade. A freshly cleaved 10 mm diameter disk of mica was applied to the cut surface of the gel. After 5−10 min, the disk was peeled off the gel surface (peel transfer) and mounted in the AFM.

Images were analyzed by software version 5.12, revision B, which is described in the Command Reference Manual supplied by the manufacturer. Length, widths, and areas were determined by particle analysis. For individual molecules adsorbed from dilute solution this process is straightforward. In the case of gels' objects of interest (OOI), that is, strands and pores, the OOI must be separated from other objects by a process called threshold segmentation. To accomplish this we chose a threshold value for pixel intensity that removed or masked the intensity of background pixels and allowed the pixel brightness of OOIs to remain undiminished. Prior to particle analysis, low-pass filtering was applied to reduce background noise and high-pass filtering was applied to highlight the OOI, which are delineated from the background as areas of rapidly changing height or phase.

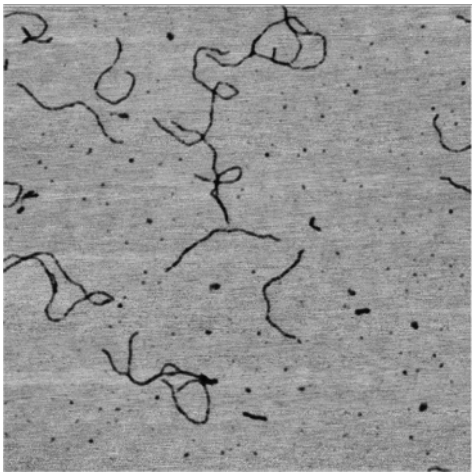

Figure 1. Height image of type 1 rat tail collagen, dissolved in 0.05 N acetic acid, concentration 0.4 μg/mL, deposited on mica, air-dried. Area shown is 1 μm^2.

Results and Discussion

To determine the accuracy of the instrument calibration, type I rat tail collagen was deposited from a 0.05 N acetic acid solution containing 0.4 μg/mL collagen. Figure 1 contains height images of individual and overlaid monomolecular collagen

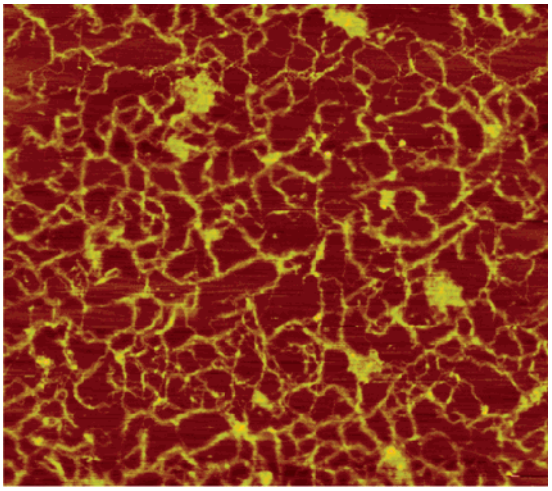

Figure 2. Height image of pectin dissolved in water, concentration 13.1 μg/mL, deposited on mica, air-dried. Pectin was prepared by microwave heating. Area shown is 1 μm^2.

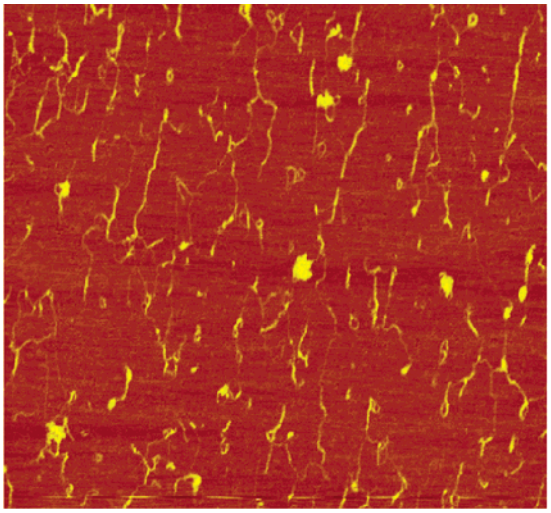

Figure 3. Height image of pectin dissolved in water, concentration 6.5 μg/mL deposited on mica, air-dried. Area shown is 1 μm^2.

molecules. The measured mean diameter of these molecules was 0.7 ± 0.2 nm. Sample size was 95 molecules. The consensus range of values for monomolecular collagen is 1.0−1.5 nm as determined over the years by various physical methods.[22−24] Possibly the lower value obtained in this study was due to a small amount of molecular compression due to probe tip−sample interaction.[25] The collagen images in Figure 1, a combination of random coils and wormlike chains, are similar to those found previously by AFM.[25]

Reliable molar mass and size characterization of macromolecules in solution by techniques such as light scattering, ultracentrifugation, membrane osmometry, and viscometry all require concentration-dependent linear extrapolations to zero concentration. In the case of polyelectrolytes, studies in water in the absence of added electrolyte are difficult to interpret because of nonlinear concentration dependence due to intra- and intermolecular charge−charge interactions. For high methoxyl pectin (HMP), a polyanion, the problem of self-interactions is compounded by the presence of multiple hydroxyl groups interspersed between carboxyl, carboxylate, methyl ester, and acetal groups. All the groups, with the possible exception of carboxylate and methyl ester groups, may be involved in the formation of hydrogen bonds. The ester may interact through hydrophobic interactions. Thus evidence indicating that HMP undergoes aggregation in water, despite the presence of negative charges, is not surprising.[4,12,13]

It has been shown by HPSEC with on-line viscosity detection[4] and repeatedly by off-line viscometry[26−28] that HMP exhibits a hyperbolic rise in intrinsic viscosity with decreasing concentration. One might expect that with decreasing concentration there would exist some concentration at which the hyperbolic viscosity curve would pass through a maximum due to the dissociation of aggregates as the concentration of dissolved pectin decreases. This could happen provided the individual molecules undergoing polyelectrolyte expansion are smaller in size than the aggregated pectin. To the best of our knowledge, the concentration range at which disaggregation occurs has not been reported for HMP in water. The concentration dependence of the specific viscosity of pectin in the presence of NaCl below 0.05 M exhibits a maximum as zero concentration of pectin is approached.[26] For this case one might postulate that polyelectrolyte expansion is suppressed by the added salt and that the maximum in specific viscosity marks the transition from aggregates to individual molecules. Figure 2 contains a height image obtained by depositing pectin on mica from an aqueous solution in which its concentration was 13.1 μg/mL. Clearly visible in that figure is network structure similar to that found for peach pectin, which previously was visualized by electron microscopy.[12,13] Also visible are dense circular areas of pectin interspersed throughout the network structure. Figure 3 contains a height image of pectin deposited on mica from water in which the concentration prior to deposition was 6.5 μg/mL. Shapes imaged included rods, segmented rods, kinked rods, rings, branched molecules, and dense circular areas of pectin. Since no network structure is visible, it appears that in the concentration range between 13.1 and 6.5 μg/mL a transition occurs from fluid networks to individual molecules or aggregates of limited size. In the case of peach pectin, microgel networks were observed at 10 μg/mL, so that for orange pectin, the transition range may start below 10 μg/mL but above 6.5 μg/mL.[12,13] Previously,[4] we suggested that the hyperbolic rise in intrinsic viscosity with decreasing pectin concentration resulted from aggregation. It also has been suggested that these increases in intrinsic viscosity resulted from polyelectrolyte expansion due to intramolecular charge−charge repulsions along the pectin chain, the so-called "polyelectrolyte effect".[26] Comparison of Figures 2 and 3 reveals that pectin chains do appear to have expanded after the network dissociated. Nevertheless, this change in size occurs at a concentration too low to measure by capillary viscometry. In fact, we expect this change in conformation of individual chains to occur when the specific viscosity decreases with decreasing concentrations. In that regime, as suggested above, the increase in specific viscosity due to the "polyelectrolyte effect" would be more than compensated for by a decrease in specific viscosity due to the dissociation of larger aggregated networks.

In Figure 4 we highlighted 100 of the longest molecules imaged in Figure 3. Table 1 contains average physical parameters of the highlighted molecules taken from five images. The mean height for the molecules was 0.43 ± 0.03 nm. For tomato pectin, the height of a "single" molecule ranged between 0.5 and 0.7 nm.[14] For the case of peach pectin extracted by sodium carbonate, cross-section analysis on a single strand gave a value of 0.2 nm.[29] If one assumes that the single pectin molecule is cylindrical and the measured width, w, is broadened by a tip with a radius of curvature (R), then the "true" molecular strand radius (r) of the molecule based on geometrical considerations is given by[30]

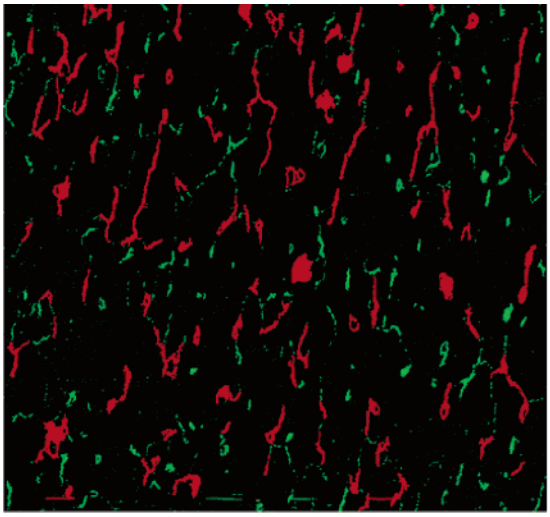

Figure 4. Height image of 100 highlighted pectin molecules dissolved in water, concentration 6.5 μg/mL deposited on mica, air-dried. Pectin was prepared by microwave heating. Area shown is 1 μm^2.

Table 1. Dimension of One Hundred Longest Pectin Molecules

dimension	mean	std dev[a]
height	0.427 nm	0.025
area	3750 nm^2	350
length	182 nm	11
width	23.0 nm	1.4

[a] Standard deviation of 100 largest molecules in five analyses.

$$r = w^2/16R \qquad (2)$$

Manufacturers' specifications for the value of R for the tips used in this study are less than 10 nm. Substituting that value for R in eq 2 and 23 nm for the value of w (see Table 1), then $2r$, the calculated maximum width of the molecule, is 6.6 nm. If one considers that the measured height is 0.43 nm, it would appear that there was lateral aggregation of as many as seven molecules.

The image in Figure 5A is the best example of a rodlike molecule. Section analysis revealed a height of about 0.56 nm (Figure 5B), a length of about 118 nm, and a width of about 14 nm. Calculating the width by eq 2 gave a corrected $2r$ value of about 2.4 nm. Comparison of the height and corrected width would indicate lateral aggregation of about four molecules.

For purposes of comparison with the pectins imaged from solution, a series of high methoxyl pectin sugar acid gels (HMSAG) were made and imaged by AFM. The gel strength was varied by changing the pH of the buffer in which the pectin and sugar were dissolved. The data in Figure 6 are a plot of gel strength at break against pH fitted to a Gaussian curve. The value of the coefficient of variance (R^2) for the fit was 0.93. AFM phase images of three of the gels plotted in Figure 6 are shown in Figure 7.

Molecular dimensions obtained by segmentation analysis of strands' phase images in Figure 7 are given in Table 2. As in a previous study,[20] we found that in many instances the gels were sufficiently flat that height images were barely visible. Nevertheless, in those instances tip−surface interactions differed greatly between the continuous interstitial pores and the strands, such that we were able capture phase shift images of the gels. In those instances geometrical tip broadening artifacts should be negligible. In many of those instances the porous interstitial phase was slightly higher than the strands so that a small amount of tip narrowing artifacts may have occurred. The data in Table 2 appear to indicate that there is no simple correlation between

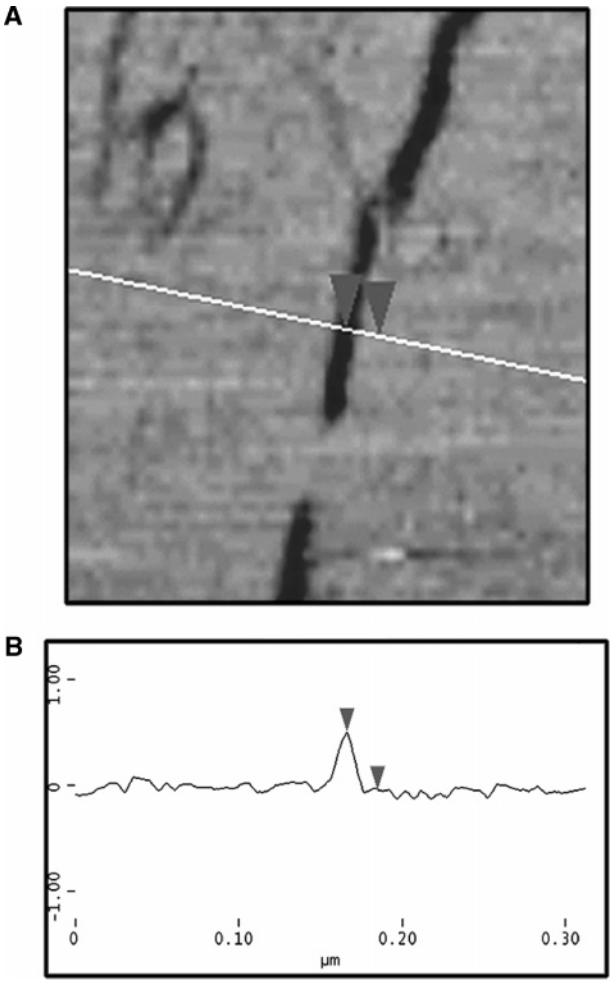

Figure 5. (A) Section analysis of pectin molecule dissolved in water, concentration 6.5 μg/mL, deposited on mica, air-dried. (B) Trace of height measurement.

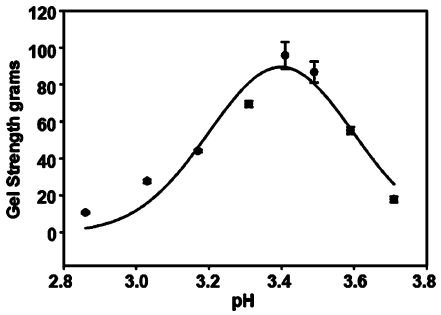

Figure 6. Gel strength dependence on buffer pH for high methoxyl sugar acid gels of pectin. Pectin was prepared by steam injection heating.

area, width, or length and gel strength. It appears from visual examination of the gel images that uniform distribution of strands and minimal space between strands may be important factors in determining gel strength. The gel in Figure 7A has a uniform distribution of strands and minimal space between strands, whereas the strands in Figure 7B are nonuniformly distributed and appear to be tangled rather than in a network structure. In Figure 7C, large strands appear to be separated by large spaces.

Figure 8A is a high-resolution phase image of the HMSAG shown in Figure 7A. Comparison of this image with the height image in Figure 2, that is, pectin networks in water with no sugar or buffer present, reveals similarity of both images.

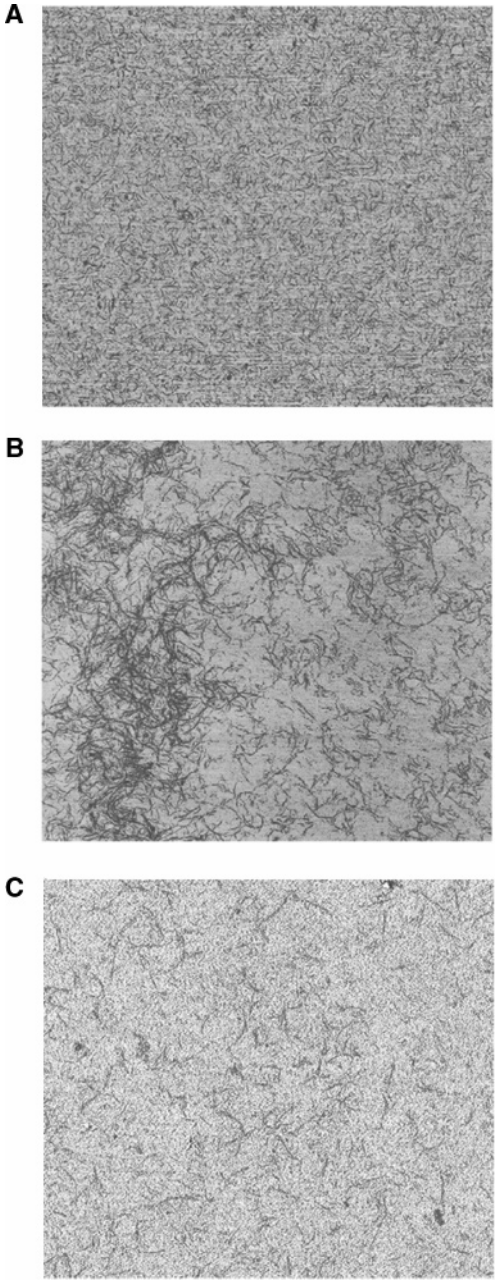

Figure 7. Phase images of high methoxyl sugar acid gels of pectin. Pectin was prepared by steam injection. A thin layer of gel was obtained on the mica by peel transfer. (A) pH 3.41, gel strength 96 g; (B) pH 3.03, gel strength 29 g; (C) pH 2.86, gel strength 11 g. Areas shown are 5 μm^2.

Table 2. Average Strand Dimensions of Pectins Gelled from Buffers with Different pH Values

pH	gel strength, g	area, nm	width, nm	length, nm
3.41	96 (8)	999 (239)	19 (6)	93 (24)
3.49	55 (13)	446 (200)	10 (5)	50 (28)
3.03	29 (1)	1453 (320)	16 (5)	74 (20)
2.86	11 (1)	516 (406)	7 (2)	36 (11)

Observation reveals that that both networks are composed of rods, segmented rods, kinked rods, rings, branched molecules, and dense circular areas of pectin. These same shapes are visible in Figure 3, dissociated pectin in water. In Figure 9, after segmentation analysis on the phase image in Figure 8, we have highlighted 100 of the largest molecules. These highlighted molecules clearly show the existence of rods, segmented rods and branched molecules observed in Figures 2−4 and 8.

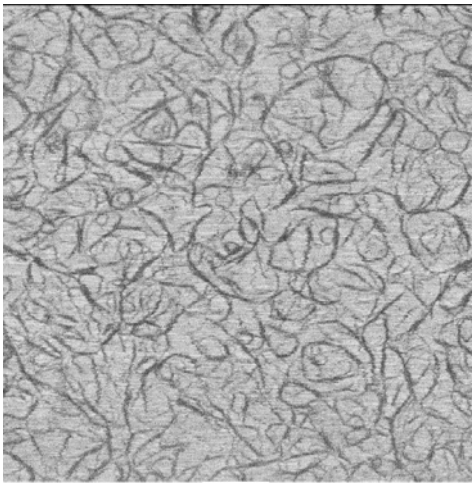

Figure 8. High-resolution phase image of high methoxyl sugar acid gel of pectin. Pectin was prepared by steam injection. A thin layer of gel was obtained on the mica by peel transfer. pH 3.41 gel strength was 96 g. Areas shown are 1 μm^2.

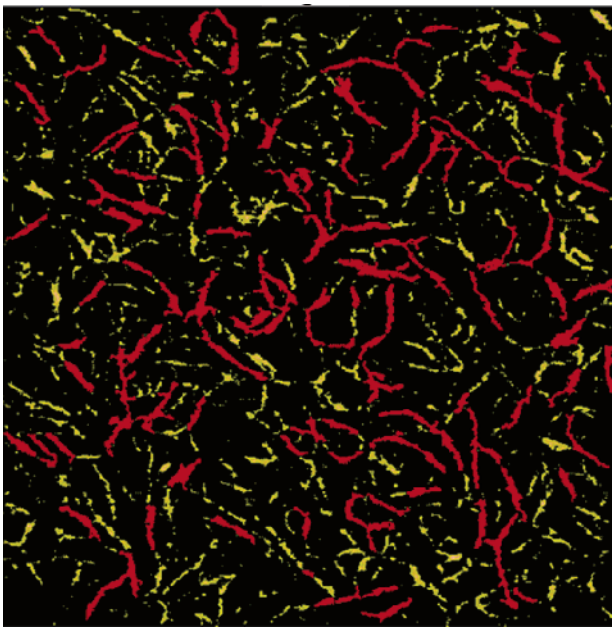

Figure 9. One hundred highlighted components obtained by segmentation analysis of highlighted components. Areas shown are 1 μm^2.

4. Conclusions

On the basis of the air-dried AFM images herein, we conclude that at concentrations greater than 10 μg/mL, orange pectin dissolved in pure water forms aggregated network structures. When the pectin concentration is 6 μg/mL or less, networks dissociate into their component parts. Also, the component parts tend to expand due to charge−charge repulsions along the chain, the so-called "polyelectrolyte effect". Nevertheless, rods, segmented rods, kinked rods, rings, branched molecules, and dense circular areas of pectin are visible. These same structures are discernible at a pectin concentration of about 13.1 μg/mL, a concentration at which pectin forms networks when dissolved in pure water, and in high methoxyl sugar acid gels of pectin. Thus one might consider pectin networks in water at concentra-

tions in excess of 10 μg/mL to be fluid precursors of high methoxyl sugar acid gels. In the latter case, the pectin in the gels may be "fixed" in a metastable state by preferential solvation of the pectin network with a high concentration of a sugar in acid buffer.[20] The networks imaged in this work are comparable to rotary-shadowed peach pectin molecules deposited on mica from water and imaged by electron microscopy.[12,13] This comparability is significant in that the network structure of pectin deposited from aqueous solution has been demonstrated for orange pectin as well as peach pectin. Furthermore, air-dried samples and rapidly dried samples under high vacuum gave comparable results. Moreover our conclusions are consistent with our previous work done in solution as referenced throughout this paper.

Acknowledgment. We thank Dr. Eleanor Brown for the gift of Type 1 rat tail collagen and helpful comments concerning the same and Ms. Halla Suleiman and Mr. André White for their technical assistance. Mention of trade names or commercial products in this publication is solely for the purpose of providing specific information and does not imply recommendation or endorsement by the U.S. Department of Agriculture.

References and Notes

(1) Vincken, J.-P.; Schols, H. A.; Oomen, R. J. F. J.; McCann, M. C.; Ulskov, P.; Voragen, A. G. J.; Visser, R. G. F. *Plant Physiol.* **2003**, 1781−1789.
(2) Carpita, N.; McCann, M. C. In *Biochemistry and Molecular Biology of Plants*; Buchanan, B., Ed.; American Society of Plant Physiologists: Rockville, MD, 2000; pp 52−108.
(3) Fishman, M. L.; Pepper, L.; Pfeffer, P. E.; Barford, R. A.; Doner, L. W. *J. Agric. Food Chem.* **1984**, *32*, 372−378.
(4) Fishman, M. L.; Gillespie, D. T.; Sondey, S. M.; Barford, R. A. *J. Agric. Food Chem.* **1989**, *37*, 584−91.
(5) Fishman, M. L.; Gross, K. C.; Gillespie, D. T.; Sondey, S. M. *Arch. Biochem. Biophys.* **1989**, *274*, 179−191.
(6) Sorochan, V. D.; Dzizenko, A. K.; Boden, N. S.; Ovodov, Y. S. *Carbohydr. Res.* **1971**, *20*, 243−49.
(7) Jordan, R. C.; Brant, D. A. *Biopolymers* **1978**, *17*, 2885−2895.
(8) Leeper, G. *J. Texture Stud.* **1973**, *4*, 248−253.
(9) Hanke, D. E.; Northcote, D. H. *Biopolymers* **1975**, *14*, 1−17.
(10) Fishman, M. L.; Pepper, L. A.; Pfeffer, P. E. In *Water Soluble Polymers*; Glass, E. D., Ed.; Advances in Chemistry Series 213; American Chemical Society: Washington, DC, 1986; pp 57−70.
(11) Chapman, H. D.; Morris, V. J.; Selvadran, R. R.; O'Neil, M. A. *Carbohydr. Res.* **1987**, *165*, 53−67.
(12) Fishman, M. L.; Cooke, P.; Levaj, B.; Gillespie, D. T.; Sondey, S. M.; Scorza, R. *Arch. Biochem. Biophys.* **1992**, *294*, 253−260.
(13) Fishman, M. L.; Cooke, P.; Hotchkiss, A.; Damert, W. *Carbohydr. Res.* **1993**, *248*, 303−316.
(14) Round, A. N.; Rigby, N. M.; MacDougall, A. J.; Ring, S. G.; Morris, V. J. *Carbohydr. Res.* **2001**, *331*, 337−342.
(15) Fishman, M. L.; Chau, H. K.; Hoagland, P.; Ayyad, K. *Carbohydr. Res.* **2000**, *323*, 126−138.
(16) Fishman, M. L.; Walker, P. N.; Chau, H. K.; Hotchkiss, A. T. *Biomacromolecules* **2003**, *4*, 880−889.
(17) Voragen, A. G. J.; Schols, H. A.; Pilnik, W. *Food Hydrocolloids* **1986**, *1*, 65−70.
(18) Yoo, S.-H.; Fishman, M. L.; Savary, B.; Hotchkiss, A. T., Jr. *J. Agric. Food Chem.* **2003**, *51*, 7410−7417.
(19) Dubois, M.; Gilles, K. A.; Hamilton, J. A.; Rebers, P. A.; Smith, F. *Anal. Chem.* **1956**, *28*, 350−356.
(20) Fishman, M. L.; Cooke, P. H.; Coffin, D. R. *Biomacromolecules* **2004**, *5*, 334−341.
(21) Kanchanasopa, M.; Manias, E.; Runt, J. *Biomacromolecules* **2003**, *4*, 1203−1213.
(22) Hulmes, D.; Miller, A. *Nature* **1979**, *282*, 878−880.
(23) Hodge, A.; Petruska, J. I. *Aspects of Protein Structure*; Ramachandran, G., Ed.; Academic Press: London, 1963; pp 289−300.
(24) Katz, E. P.; Li, S. *J. Mol. Biol.* **1973**, *73*, 351−369.
(25) Bozec, L.; Horton, M. *Biophys. J.* **2005**, *88*, 4223−4231.
(26) Pals, D. T. F.; Hermans, J. J. *Recl. Trav. Chim.* **1952**, *71*, 433−457.
(27) Michel, F.; Thibault, J. F.; Doublier, J.-L. *Carbohydr. Polym.* **1984**, *4*, 283−297.
(28) Yoo, S.-H.; Fishman, M. L.; Hotchkiss, A. T., Jr.; Lee, H. G. *Food Hydrocolloids* **2005**, *20*, 62−67.
(29) Yang, H.-S; Feng, G.-P; An, H.-J; Li, Y.-F. *Food Chem.* **2006**, *94*, 179−192.
(30) Morris, V. J.; Gunning, A. P.; Kirby, A. R.; Round, A.; Waldron, K.; Ng, A. *Int. J. Biol. Macromol.* **1997**, *21*, 61−66.

BM0607729